REPORT DOCUMENTATION PAGE

Form Approved
OMB No. 0704-0188

1. REPORT DATE (DD-MM-YYYY)	2. REPORT TYPE	3. DATES COVERED (From - To)
	Technical Papers	

4. TITLE AND SUBTITLE — Please see attached

5a. CONTRACT NUMBER

5b. GRANT NUMBER

5c. PROGRAM ELEMENT NUMBER

6. AUTHOR(S)

5d. PROJECT NUMBER 2308

5e. TASK NUMBER M13C

5f. WORK UNIT NUMBER 346057

7. PERFORMING ORGANIZATION NAME(S) AND ADDRESS(ES)

Air Force Research Laboratory (AFMC)
AFRL/PRS
5 Pollux Drive
Edwards AFB CA 93524-7048

8. PERFORMING ORGANIZATION REPORT

9. SPONSORING / MONITORING AGENCY NAME(S) AND ADDRESS(ES)

Air Force Research Laboratory (AFMC)
AFRL/PRS
5 Pollux Drive
Edwards AFB CA 93524-7048

10. SPONSOR/MONITOR'S ACRONYM(S)

11. SPONSOR/MONITOR'S NUMBER(S) Please see attached

12. DISTRIBUTION / AVAILABILITY STATEMENT

Approved for public release; distribution unlimited.

13. SUPPLEMENTARY NOTES

14. ABSTRACT

20030116 062

15. SUBJECT TERMS

16. SECURITY CLASSIFICATION OF:			17. LIMITATION OF ABSTRACT	18. NUMBER OF PAGES	19a. NAME OF RESPONSIBLE PERSON
a. REPORT	b. ABSTRACT	c. THIS PAGE			Leilani Richardson
Unclassified	Unclassified	Unclassified	A		19b. TELEPHONE NUMBER (include area code) (661) 275-5015

Phase Doppler Interferometry with Probe-to-Droplet Size Ratios Less Than Unity Part II: Application of the Technique

P. A. Strakey* & D. G. Talley
Air Force Research Laboratory, AFRL/PRSA, 10. E. Saturn Blvd., Edwards AFB, CA 93524

S. V. Sankar & W. D. Bachalo
Consultants, 14660 Saltamontes Way, Los Altos Hills, CA 94022

Abstract

Practical limitations associated with the use of small probe volumes for measuring large droplets with the phase Doppler interferometry technique are discussed. An intensity validation scheme and corresponding probe volume correction factor have been developed that reject trajectory errors and account for the rejections in calculation of the probe cross-sectional area. The intensity validation scheme also provides a tractable method of setting the photomultiplier tube gain and laser power. Volume flux measurements in dilute sprays have shown a significant improvement over standard phase Doppler interferometry techniques at small beam waist to droplet size ratios.

Introduction

Phase Doppler interferometry, which is a single particle counting technique requires that the probe volume, defined by the laser beam waist and spatial filter, be made small enough to ensure that only one droplet is present in the probe volume at any given time. For sprays in which both the droplet number density and droplet sizes are relatively large, the laser beam waist must often times be made smaller than the maximum droplet size being measured. While there is no fundamental restriction on this approach, there are however several issues that arise when measuring droplets larger than the probe diameter. One of the most arduous problems of the PDI technique when the droplet size becomes comparable to, or smaller than the probe diameter has been referred to as trajectory error. This is the issue that has also received the most attention in the literature in the past several years [1,2]. It has been demonstrated that accurate size measurements can be made at probe to droplet size ratios, D_w/D as small as 0.17 [1]. It has also been demonstrated that trajectory errors due to reflective contributions to the scattered light signal can be eliminated with a combination of a 3-detector phase ratio criteria and an intensity validation technique [1]. The phase ratio validation criteria using a non-integer detector separation ratio has been shown to eliminate large droplets being erroneously reported as smaller droplets. The intensity validation criteria prevents small droplets from being measured as much larger droplets. It has also been shown that intensity validation provides a simple and robust method of measuring the probe cross sectional area, which is needed for calculation of the spray mass flux.

Along with trajectory errors, there are a number of other potential problems that arise when the probe diameter and slit size are made much smaller than the droplet size of interest. Some of the issues that must be addressed include;

i) instrument limitations for short Doppler burst times.
ii) signal visibilty effects.
iii) probe volume correction factors appropriate for large droplet to probe size ratios.
iv) phase variance as droplets pass through the probe volume.

* To whom correspondence should be addressed

Each of these issues will be addressed in the following sections with the intent of providing a sound methodology for applying the small probe volume PDI technique in realistic spray environments.

Transit Time Limitations

Without having the ability to measure multiple particles in the probe volume, it is necessary that the size of the probe volume be reduced until the probability of finding multiple particles within the probe volume is negligibly small. In effect, the probe volume can theoretically be made much smaller than the size of the droplet being measured as demonstrated by Haugen *et al.* [3]. For sizing non-absorbing droplets, the forward scattering region is advantageous in maximizing light scattering intensity and minimizing sizing errors due to the presence of unwanted scattering modes such as external reflection. In the forward scattering region, refracted light is used for droplet sizing. The refracted light reaching the receiving optics originates from a very small area on the face of the drop, as illustrated in Figure 1. All other rays incident on the droplet are refracted elsewhere, thus it is not necessary to illuminate the entire droplet. In essence, this small area on the droplet surface acts as a lens which magnifies and projects an image of the fringe pattern onto the receiver lens. The resultant magnified fringe spacing is measured as a phase shift between the detectors and, for pure refraction, is linearly proportional to the droplet size. The probe size could theoretically be made as small as or smaller than the size of the projected area on the droplet surface.

The size and shape of the projected area on the surface of the droplet is a function of the receiving optics, and for the Aerometrics PDPA system with f5.0 receiving optics, the width in the scattering plane of the projected area is approximately 10% of the droplet diameter. The height of the projected area is somewhat less, since the light entering the receiving lens is directed to one of three detectors. The shape of the detector apertures is roughly rectangular with an aspect ratio (width to height) of approximately 2.5 for detectors 1 and 3 and an aspect ratio of 4.5 for detector 2. Therefore, the projected area of a 300 μm droplet would be a rectangular area on the front surface of the droplet 30 μm wide in the scattering plane, by 12 μm normal to the scattering plane for detector 1.

The detected scattered light from the projected area, also referred to as the interrogation region, will be the average intensity and phase over this region. In theory, the resulting phase should vary only slightly over this region due to the slight change in scattering angle. As the diameter of the probe beams approaches the size of the interrogation region on the droplet surface the resulting intensity will, however, vary significantly due to the Gaussian intensity profile of the probe beams. The detected intensity will be proportional to the average incident intensity over the interrogation region. This does not, however, pose a fundamental limitation on the minimum useable probe beam diameter.

The minimum usable probe diameter is limited by the droplet transit time and the maximum sampling rate of the instrument. For the Aerometrics DSA, which is an FFT based system, Ibrahim *et al.* [4] has shown that the rms phase measurement error is inversely proportional to the square root of the sample size. At a signal-to-noise ratio of 0 dB, the rms phase error for a 3 detector configuration was measured to be 1.8° for a sample size of 128. A sample size of 32 would thus have a rms phase error of 3.6°. Currently the DSA has a maximum sampling rate of 160 MHz. This would yield a minimum transit time of 0.2 μsec for a sample size of 32. The burst detector also requires a finite amount of time in which to trigger the sampling gate. A minimum 16 point FFT would require 0.1 μsec to trigger the gate on a Doppler burst. Because the burst detector and signal measurement electronics use an overlapping sampled data set, the burst detector does not increase the signal duration necessary for measurement, which would still be 0.2 μsec. For a droplet traveling on a trajectory in which the interrogation region would pass through the center of a 60 μm probe diameter, the maximum velocity for size measurement would be 300 m/s. The practical maximum velocity would be somewhat lower for droplets passing through the edge of the probe volume, where the detectable path length would be shorter by a factor of about two at the $1/e^2$ probe diameter. Thus, the maximum velocity which would provide detectability over the entire beam cross section as defined by D_w for a moderately sized droplet would be 150 m/s, well within the range of most spray applications. Very small droplets will have an effective probe diameter smaller than D_w due to limitations on signal triggering

within the DSA and may only be detectable for trajectories through the center of the probe volume, as will be discussed later.

Signal Visibility Effects

Another concern when measuring droplets that are very large with respect to the fringe spacing is signal visibility for the refractively scattered light. A typical Doppler burst signal from a moderately sized droplet with a signal visibility of 0.5 is shown in Figure 2. The visibility, as defined by Equation 1, is a function of I_{max} and I_{min} which are the maximum and minimum amplitudes of the raw Doppler burst signal.

$$Vis = \frac{I_{max} - I_{min}}{I_{max} + I_{min}} \tag{1}$$

For small droplets with an interrogation region much smaller than the fringe spacing, the visibility will be nearly one, meaning that the Doppler burst signal will have a maximum amount of signal modulation. This is important because the Doppler burst signal is high-pass filtered in the DSA to remove the DC pedestal component before sampling. As the droplet size increases and the interrogation region approaches the fringe spacing, the refractive visibility approaches zero. The reflective visibility, however, will still be very large because the interrogation spot size for reflection is much less than that for refraction. Thus, for a large droplet, even though the absolute magnitude of scattered light intensity might be much larger for refraction than reflection, the resultant signal modulation resulting from the coherent interaction of the two scattering modes will be dominated by reflection. This phenomenon will affect PDI measurements with large probe diameter to droplet size ratios as well as small ratios. It is important that the refractive signal visibility does not approach zero over the droplet size range of interest. Refractive visibility can be increased by decreasing the beam intersection angle, which increases the fringe spacing, or by decreasing the size of the detector aperture in the direction normal to the plane of scattering for standard PDI systems.

Temporal Phase Variance

Several theoretical studies have shown that the phase of a scattered light signal will vary as a function of droplet location along a given trajectory as well as with the location of the trajectory [5,6]. This holds true even for trajectories normal to the scattering plane [6]. As a droplet passes through the probe volume normal to the scattering plane, the location of the interrogation region for refraction (p=1) and reflection (p=0) with respect to the center of the probe volume, changes as a function of location along the trajectory. As the location of each of the interrogation regions changes, so does the relative scattering intensity of each scattering component. This results in a phase that changes slightly as the droplet passes through the probe volume. The geometric optics model described in Part I of this paper was used to study this effect by varying the droplet trajectories within the 10:1 intensity defined probe volume while calculating the maximum phase variation as the droplets traversed the probe volume. Calculation were performed from z = 30 to -30 μm, where z is the trajectory coordinate normal to the scattering plane.

It was found that the maximum variance in the phase shift always occurred for detectors *1* and 2, and always occurred for trajectories along the edge of the probe volume farthest from the receiver. This is what one might expect, since this is the trajectory where reflective contributions to the total scattered light signal are maximized. Figure 3 is a plot of the variance in φ_{12} expressed as a percentage of the average φ_{12} as a function of droplet diameter for the optical configuration of case 1 given in Table 1. Droplets much smaller than the probe diameter display very little phase variance as a result of the nearly uniform illumination of these small droplets. As droplet size approaches the probe diameter, the relative reflective contribution increases for trajectories along the far edge of the beam waist, which causes an increase in the phase variation as the droplet traverses the probe volume. As the droplet size further increases, the reflective contribution begins to decrease because the reflective and refractive interrogation areas are beginning to separate in space and in intensity. As a result, for droplets much larger than the beam diameter, there are only refractive dominated or reflective dominated trajectories. Within the 10:1 intensity range, there are

only refractive dominated trajectories. For droplets larger than about 100 μm there is again an increase in phase variance which is probably due to the large variation in illumination intensity over the refractive interrogation region which is approaching the beam waist diameter.

The effect of phase variance on the response of the instrument is strongly dependent on the duration of the sampled Doppler burst and the droplet velocity. For a minimum sample time of 0.2 μsec and a droplet velocity of 150 m/s, the maximum sampled path length would be 30 μm, which is less than the 60 μm path length shown in Figure 3. Since the phase variance is fairly linear with path length, the maximum variation in φ_{12} for a 60 μm droplet would be (30 μm/60 μm)·15%, which is equal to 7.5%. This small variation in phase over the sampled burst would slightly decrease the signal to noise ratio of the Fourier transformed signal, but would not cause a substantial measurement error.

Probe Volume Correction (PVC)

Conventional PVC

Due to the nature of the Gaussian intensity distribution at the probe volume and the fact that droplets much larger than the wavelength of light scatter light in proportion to the droplet diameter squared, the cross sectional area of the probe volume varies with the particle diameter being measured [7]. Larger particles will scatter more light and therefore be detected further out from the center of the probe volume than smaller particles. A correction factor, known as the probe volume correction (PVC) is employed in the DSA software and takes this into account. The current PVC is based on either an analytical correction or a transit time correction which measures the maximum path length for each particle size class and assumes that this length is equal to the maximum probe diameter for that size class. The "corrected" number of counts in each size class is calculated as;

$$n_c(D) = n(D) \cdot \left(\frac{L_{max}}{L(D)} \right) \tag{2}$$

where L_{max} is the maximum path length through the probe volume, which occurs for the largest droplet size class, and L(D) is the measured maximum path length for each size class [8]. This PVC does not, however, take into account the decrease in the width of the probe volume when intensity validation is used to "clip" the edges of the probe volume ~~in order~~ to eliminate trajectory dependent scattering errors. A new PVC based on the estimated diameter of the probe volume for each size class at the minimum intensity cutoff is therefore needed.

Signal Dynamic Range and Intensity Based PVC

In a typical spray, the range of measured droplet sizes can be quite large. The Aerometrics PDPA is capable of sizing droplets over a dynamic size range of 50:1, with the limit being the dynamic range of the photomultiplier tubes (PMT's) and detection electronics. The dynamic range is bounded by signal saturation on the PMT's and the minimum signal which can be measured at a fixed signal-to-noise ratio. Ibrahim *et al.* [4] have shown that the DSA is capable of making reliable phase measurements at signal-to-noise ratios as low as -10 dB. The use of a 10:1 intensity validation criteria within each size class would produce an intensity dynamic range of 25,000 to 1. The DSA is currently only capable of measuring a scattered light intensity range of 1,000 to 1.

The dynamic range limitation can be overcome by setting the maximum intensity of a droplet one-third the maximum measurable droplet size to just saturate the detector (500 mv). For the optical configuration of case1 in Table 1 and a droplet size range of 50:1, the maximum droplet size is 310 μm for water droplets in air. Droplets larger than 103 μm will tend to saturate the instrument with a 310 μm droplet having a theoretical maximum scattering intensity of 4,500 mv. It is not important that we know the intensity of

these larger droplets, only that we know that their scattering intensity is above 450 mv, which is the 10:1 lower intensity cutoff for this size class. It should be pointed out that signal saturation does not degrade the signal-to-noise ratio or the accuracy of the phase measurement.

The smallest measurable droplet size of 6.2 μm (for a 50:1 range) would yield a maximum scattering intensity of 1.8 mv. The minimum measurable intensity is about 0.5 mv, but the minimum intensity required to produce an instrument trigger is 1 mv. For droplet sizes with a scattering intensity less than 1 mv within the probe volume defined by a 10:1 intensity range a correction factor must be employed which accounts for the reduced probe cross-sectional area over which measurements may be made. For the optical configuration studied here, a 14.6 μm droplet would produce a maximum scattering intensity of 10 mv. For droplets in the size range of 6.2 to 14.6 μm, a probe volume correction factor must be employed. The diameter of the probe volume for droplets in this size range is simply the diameter of the Gaussian probe beam at which the scattering intensity equals 1 mv.

Assuming a Gaussian intensity distribution in the probe volume, the width of the beam waist at the lower cutoff point (D_w') can be calculated. The Gaussian intensity distribution at the beam waist is given by Equation 3;

$$\frac{I}{I_o} = \exp\left[\frac{-8y'^2}{D_w^2}\right] \tag{3}$$

Where I_o is the intensity at the center of the beam waist and y' is the distance from the center normal to the beam propagation direction. For the present optical configuration (case 1, Table 1), $D_{w10\%}$ = 64 μm. With a 14.6 μm droplet producing a peak scattering intensity of 10 mv, the probe diameter at the 1 mv detection limit would be;

$$D_w' = \left[\frac{-D_w^2}{2}\ln\left(\frac{21.32}{D^2}\right)\right]^{\frac{1}{2}} \qquad D < 14.6\mu m\ . \tag{4}$$

For droplets larger than 14.6 μm, D_w' is fixed at 64 μm. A plot of the probe diameter calculated from the intensity cutoff scheme (Equation 4) and the currently employed analytical PVC from the Aerometrics software is shown in Figure 4. The intensity based probe volume is constant at 64 μm for droplets between 14.6 μm and 310 μm. For smaller droplets Equation 4 is used. The analytical PVC currently employed in the DSA software has a probe diameter continuously increasing with droplet size.

Implementation of Intensity Validation

The intensity validation technique can be implemented by setting the maximum intensity to be at saturation (500 mv) for a particle size equal to one third the maximum measurable size (103 μm). The maximum intensity line then follows an $I \propto D^2$ relationship for the other particle size classes.

The PMT voltage must be set above 400 volts to insure that the PMT's respond linearly with scattered light intensity. Linearity was verified experimentally with the mono-dispersed droplet experiments. The DSA software employs an intensity validation setup page in which data can be collected and a plot of diameter verses the square root of intensity is displayed. Laser power or PMT voltage can then be adjusted until the maximum intensity reading in each size class falls upon the upper intensity cutoff line. Data can then be collected and post-processed to reject particles in each size class with an intensity less than 10% of the maximum intensity. The PVC described above can then be employed to account for the smaller probe

diameter for droplets less than 14.6 μm in diameter. The probe cross-sectional area is then calculated with Equation 5 using the probe diameter, as given in Fig. 4.

$$A = \frac{D_w' \cdot D_s}{\sin(\theta)} \quad (5)$$

The corrected number of counts for each size class is given by Equation 6,

$$n_c(D) = n(D) \cdot \left(\frac{A_{D_{w10\%}}}{A} \right) \quad (6)$$

where $A_{Dw10\%}$ is the probe area calculated with the beam waist diameter (64 μm) at the lower intensity cutoff for droplets larger than 14.6 μm in diameter.

Another benefit of this technique is that it provides a tractable method for setting the PMT voltage and laser power. Several studies have been done in the past which show a sensitivity of the measurement to the PMT voltage setting at a given laser power [7,9]. The informational feedback of the intensity validation method allows the user of the instrument to pre-select an upper intensity verses diameter relationship and set the PMT voltage to match that relationship.

The intensity validation scheme described herein was calculated for a particular size range corresponding to the optical configuration used in this study. A similar PVC could be generated for any size range of 50 to 1 or less, as long as the saturation point is set for a droplet one-third the maximum measurable droplet size.

Spray Measurements

Using the 10:1 intensity validation scheme and associated PVC, measurements in a dilute water spray were performed to demonstrate the technique. The PDI instrument used in this study was the same as described in Part I of this paper. The spray was formed by a Delavan WDB10-45° nozzle operated at 0.34 MPa and at atmospheric back-pressure. Measurements of droplet size, velocity and volume flux were made as a function of radial position in the spray at a location of 10 cm downstream of the injection point. Measurements were made with both the current small probe volume configuration (case 1, Table 1) and a more "conventional" probe volume (case 2, Table 1), with and without intensity validation. Measurements of volume flux are presented in Figure 5 along with the volume flux measured with a collection tube. The accuracy of the collection tube measurement was assessed by integrating the radial flux profile and comparing it to the measured injected flowrate. The integrated collection tube measurement was 8% lower than the measured injected flowrate. As can be seen in the figure, without intensity validation, the PDI measured volume flux is much larger than the collection tube measurement, even with the larger probe volume. This is a result of small particles passing through the edges of the probe volume and being erroneously measured as much larger particles, thus greatly adding to the measured volume flux. Good agreement between the collection tube measured volume flux and the volume flux measured with the small probe volume and 10:1 intensity validation scheme can be seen in Figure 5. Although these experiments were conducted with a detector separation ratio of 2.96 which would allow droplets larger than 150 μm to be measured as smaller droplets, the maximum valid droplet size was just under 150 μm. For this case, intensity validation alone would be sufficient to reject erroneous measurements.

Figure 6 is a scatter plot droplet diameter verses the square root of the scattered light intensity for the radial position of 0.0 mm. Figure 6 is similar to what is viewed with the DSA software. Also shown are the high and low intensity lines. The suspect particles are those larger than about 150 μm, which show only low scattering intensities. Figure 6 also reveals another important advantage to using intensity validation which is the ability to detect multiple droplet occurrences in the probe volume. For single droplet occurrences, a

sharp cutoff in the data near the maximum scattering line would be observed, as is seen in Figure 6. Since two or more droplets coincident in the probe volume would scatter significantly more light, multiple droplet occurrences would show up as a scattering in the data at intensities greater than the upper intensity line.

Figure 7 is a histogram of the relative volume concentration for the radial location of 0.0 mm with and without intensity validation, demonstrating the significant change in volume distribution in a real spray when trajectory dependent errors are eliminated. It is interesting that even with a maximum droplet size of 150 μm, the mass flux measured with the 352 μm probe diameter (Fig. 5) was still significantly greater than the mass flux measured with the collection tube. This could be a result of the slit effect discussed in Part I of this paper which showed an increase in the number of measurement errors when the slit was accounted for with the larger beam waist diameter.

Conclusions

Although there are certain practical limitations on minimum useable probe diameter, current FFT based detection schemes are quite capable of making accurate droplet size measurements for relatively small probe diameters and high flow velocities. Optical limitations such as signal visibility can be overcome by proper selection of the beam crossing angle or detector aperture. Droplets much larger than the beam waist can be measured when a combination of phase ratio and intensity based validation criteria are used. An intensity based probe volume correction factor has also been shown to provide a simple and robust way to calculate the probe cross-sectional area. The implementation of the technique also provides a tractable method for determining the appropriate laser power and PMT voltage during an experiment. Measurements in dilute sprays have demonstrated that the technique is capable of rejecting trajectory dependent scattering errors while greatly improving the accuracy of liquid flux measurements.

Acknowledgement

The authors would like to thank Mr. Mike Griggs for his assistance in operating the facility and conducting experiments.

References

1. P. A. Strakey, D. G. Talley, S. V. Sankar and W. D. Bachalo, "Phase Doppler Interferometry with Probe-to-Droplet Size Ratios Less Than Unity Part I: Trajectory Errors"

2. S. V. Sankar and W. D. Bachalo, "Performance Analysis of Various Phase Doppler Systems", *4th International Congress on Optical Particle Sizing*, Nuremberg, Germany, March 21-23, 1995.

3. Per Haugen, Edward I. Yayes, Hans-Henrik von Benzon, "Size and Velocity Measurements of Large Drops in Air and in a Liquid-Liquid Two-Phase Flow by the Phase-Doppler Technique", *Part. Part. Syst. Charact.*, Vol. 11, pp. 63-72, 1994.

4. K. M. Ibrahim, G. D. Werthimer and W. D. Bachalo, "Signal Processing Considerations for Laser Doppler and Phase Doppler Applications", Presented at the *5th International Symposium on the Application of Laser Techniques of Fluid Mechanics*, Lisbon, Portugal, July 9-12, 1990.

5. Y. Hardalupus and C. H. Liu, Implications of the Gaussian Intensity Distribution of Laser Beams on the Performance of the Phase Doppler Technique. Sizing Uncertainties", *Prog. Energy Combust. Sci.*, Vol. 23, pp. 41-63, 1997.

6. Gerard Grehan, Gerard Gouesbet, Amir Naqwi and Franz Durst, "Trajectory Ambiguities in Phase Doppler Systems: Study of a Near-Forward and Near-Backward Geometry", *Part. Part. Syst. Charact.*, Vol. 11, pp. 133-144, 1994.

7. W.D. Bachalo, R.C. Rudoff and A. Brena de la Rosa, "Mass Flux Measurements of a High Number Density Spray System Using the Phase Doppler Particle Analyzer", *AIAA 88-0236, 26th Aerospace Sciences Meeting*, Jan. 11-14 1988.

8. Aerometrics Phase Doppler Particle Analyzer Doppler Signal Analyzer, 1-Component User's Manual, Release 1.0, Appendix B, April 1993.

9. Chien-Pei Mao, "Measurements of Sprays Using Phase Doppler Instruments: A Study to Establish Formal Operating Procedures", Presented at the *9th Annual Conference on Liquid Atomization and Spray Systems*, May 19-22, San Francisco, CA, 1996.

Nomenclature

A	probe cross-sectional area (μm^2)
C	number of counts
C_c	corrected number of counts
D	droplet diameter (μm)
D_s	apparent slit width (μm)
D_w	$1/e^2$ beam waist diameter (μm)
$D_{w10\%}$	probe diameter at $1/10^{th}$ of I_{max}(μm)
D_w'	probe diameter (μm)
I	intensity
I_o	intensity at beam center
I_{max}	maximum signal intensity
I_{min}	minimum signal intensity
L_{max}	maximum path length (μm)
$L(D)$	path length (μm)
N	droplet dumber density (cc^{-1})
y'	distance from center of beam waist (μm)
φ	phase difference
θ	scattering angle

Subscripts

12	denotes detectors 1 and 2
13	denotes detectors 1 and 3

Table 1 : Optical configuration for experiments and model calculations.

	Case 1	Case2
Beam Separation (mm)	21	20
Transmitter Focal Length (mm)	470	500
Receiver Focal Length (mm)	500	500
Scattering Angle (deg)	30	30
Initial Beam Diameter (mm)	9.6	2.0
$1/e^2$ Beam Waist Diameter (μm)	60	352
Slit Width (μm)	50	100
Receiver Magnification	2.0	2.0
Receiver Lens Diameter (mm)	105	105
Laser Wavelength (nm)	514.5	514.5
Fringe Spacing (μm)	11.52	12.87
S_{12} (mm)	23.34	23.34
S_{13} (mm)	69.00	69.00
S_{13}/S_{12}	2.96	2.96
Sample Rate (MHz)	160	40
Sample Size	64	64
Threshold (mv)	3.0	3.0

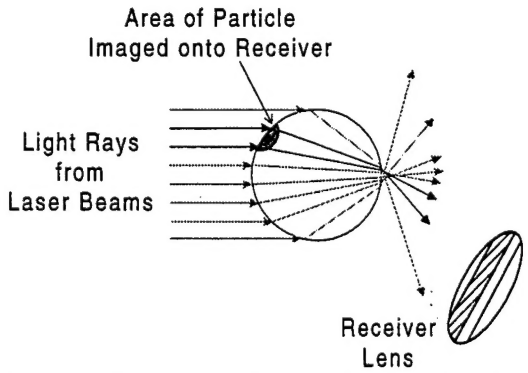

Figure 1: Illustration of ray paths reaching the receiver lens.

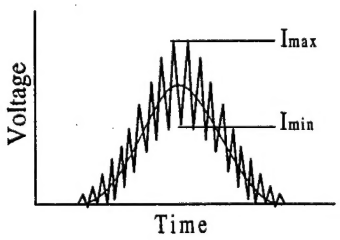

Figure 2: Typical Doppler burst signal with a visibility of 0.5.

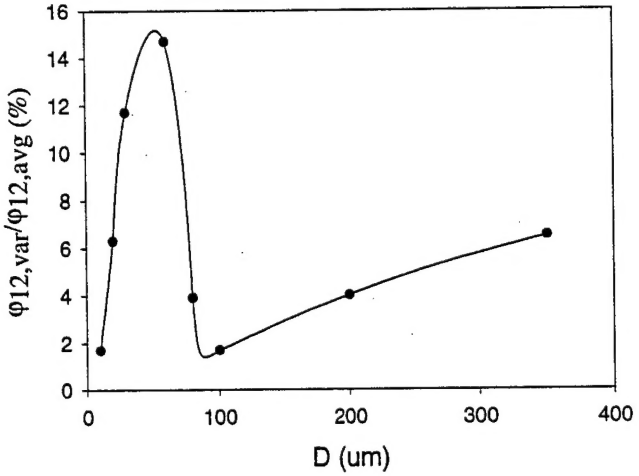

Figure 3: Maximum phase variance expressed as a percentage of the average phase from detectors 1-2 as a function of droplet diameter. Optical configuration of case 1, Table 1.

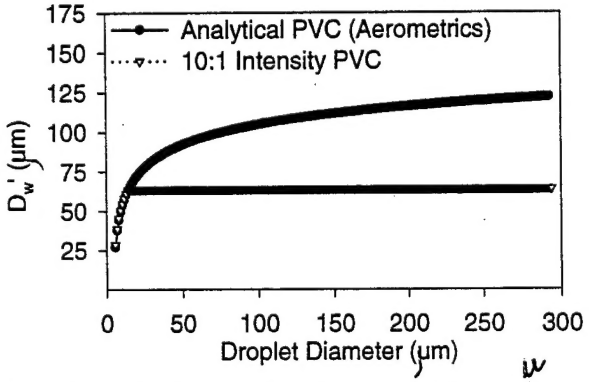

Figure 4: Calculated probe diameter (D_w') verses droplet diameter; analytical PVC and 10:1 intensity PVC.

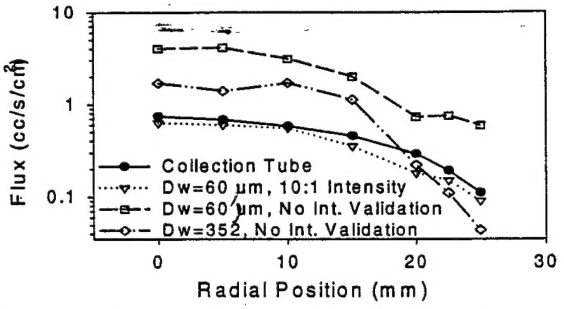

Figure 5: Volume flux vs. radial position, Delavan WDB10-45°, P=0.34 MPa, Z=10 cm.

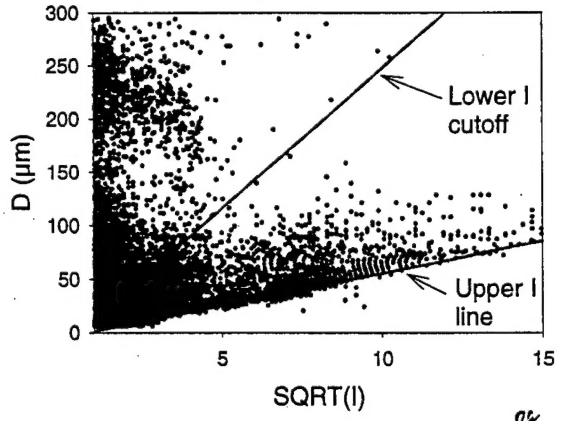

Figure 6: Scatter plot of droplet diameter vs. Square root of intensity, Delavan WDB10-45°, P=0.34 MPa, Z=10 cm, r=0.0 mm.

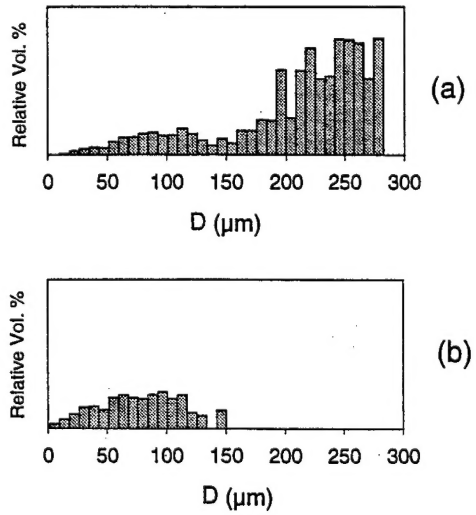

Figure 7: Histograms of relative volume percentage, Delavan WDB10-45°, P=0.34 MPa, Z=10 cm, r=0.0 mm; (a) without intensity validation and (b) with intensity validation.